Static and energetic fracture parameters for rocks and concretes

A. Carpinteri ([1])

The object of the paper is to determine the fracture toughness parameters K_{IC}, $\mathcal{G}_{IC}$ and J_{IC} for some aggregative materials. Values of the J-integral are calculated from load-displacement curves, following the procedure suggested by Begley and Landes for steel alloys. Some recurring experimental incoherences are explained applying Buckingham's Theorem for physical similitude and scale modeling to Fracture Mechanics. Thus a non-dimensional parameter can be defined (the test brittleness number), which governs the fracture-sensitivity phenomenon. The fracture parameters K_{IC} and J_{IC} are connected by a fictitious Young's modulus E^*, which is lower than the real modulus E and represents the stiffness of the damaged material near the crack tip before the extension. When the specimen sizes are so small that the material becomes fracture insensitive, then E^* appears higher than E.

1. INTRODUCTION

This paper aims at presenting the experimental determination of the following critical fracture toughness parameters:

1) stress-intensity factor K_{IC} [1];
2) crack extension force $\mathcal{G}_{IC}$ ([1], [2]);
3) integral J_{IC} ([3], [4]),

relating to a Carrara marble, a mortar and two concretes with aggregate of different maximum size. The main purpose is to study the statistical fluctuations of the results and to clarify the connection between the above-mentioned experimental parameters. Namely K_{IC} is a static parameter, directly attainable by the structure and crack geometry and by the fracture load, while $\mathcal{G}_{IC}$ and J_{IC} are energetic parameters representing the work necessary to have a unit fracture surface. It will be shown how the "force" K_{IC} and the "energy" J_{IC} are connected by a "stiffness" E^*, probably representing Young's modulus of the damaged material near the crack tip before the extension.

In the last few years a great effort has been made to verify the range of applicability of the J-integral to the metallic materials, but a similar effort has not been made to clarify limitations and advantages of J applications to aggregative materials. The J values have hereby been calculated following the procedure suggested by Begley and Landes [5] for the high strength steel alloys.

The most worrying problem connected with fracture testing is the uncertainty of the reproducibility for the crack propagation phenomenon, varying the shape and/or the size of the cracked structure. While the techniques to obtain the fracture toughness parameters have rapidly been developed and, as far as the metallic materials are concerned, have already been standardized [6], it is still not completely clear today how far it is possible to extrapolate the laboratory results to the project of structures of large sizes and complex shape. In fact several authors observed an ample variability of the fracture toughness parameters, varying the specimen geometry and the specimen size ([7]. . .[27]). Some notes on this problem will be given afterwards by a Dimensional Analysis application.

([1]) Universita' di Bologna, Facolta' di Ingegneria, Istituto di Scienza delle Costruzioni, Viale Risorgimento, 2, 40136 Bologna (Italy).

0025-5432/1981/151/ $ 5.00/

2. MATERIAL AND SPECIMEN DESCRIPTION

One of the essential requisites that the author applied to the tests was simplicity, naturally in addition to reliability.

The *three point bending test* was chosen as test geometry, i.e. beams with rectangular cross-section, notched and loaded in the middle. Four series of three point bending tests were performed using 18 specimens ($10 \times 10 \times 30$ cm) of Carrara marble, 15 specimens ($15 \times 15 \times 60$ cm) of mortar, 21 specimens ($15 \times 15 \times 60$ cm) of a concrete with maximum aggregate size 9.52 mm and 21 of a concrete with maximum aggregate size 19.10 mm.

The considerable specimen size allowed a higher notch sensitivity: the crack propagation namely preceded (mortar) or interacted (marble and concretes) with the material micro-cracking and the paste-aggregate debonding.

The span was 28 cm for marble beams and 55 cm for the other materials.

Mortar had the weight ratios (water/cement)=0.4 and (sand/cement)=2.05. The maximum size of sand was 2.38 mm. The first concrete (1) had ratios: (water/cement)=0.5, (sand/cement)=2.46 and (aggregate/cement)=2.89. The second concrete (2): (water/cement)=0.6, (sand/cement)=2.16 and (aggregate/cement)=2.34. After casting the specimens were mixed in a high speed mixer in order to avoid voids and inhomogeneities.

Two specimen sections after testing are shown in figure 1.

For every notch depth three similar specimens were prepared. For every material three specimens were not notched, in order to determine the ultimate strength σ_u and Young's modulus E (table I). The notch was performed on the smooth side of the specimen, corresponding to a lateral side of the casting mould, by a circular saw of 2 mm thickness. In the marble specimens the notches were cm 1, 2, 3, 4, 5 deep; in the mortar specimens cm 1.5, 3.0, 4.5, 6.0; in the concrete specimens cm 1, 2, 3, 4, 5, 6.

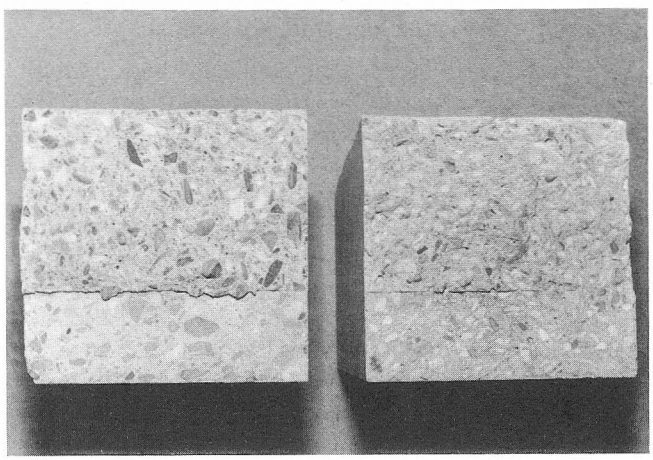

Fig. 1. – Specimen sections after testing, relating to the two tested concretes.

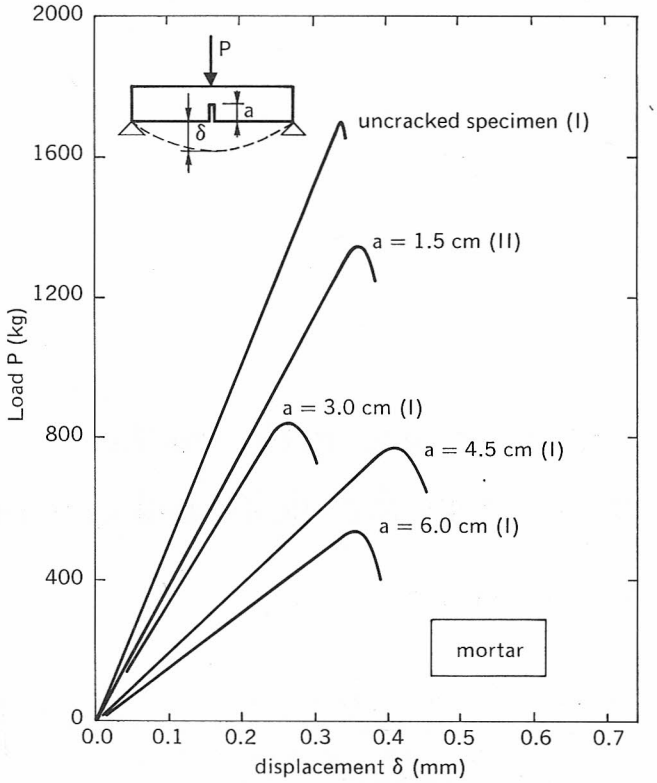

Fig. 2. – Load-displacement diagrams for mortar specimens.

The notched specimens were subjected to a monotonic loading process by a hydraulic testing machine. The load and displacement transducer outputs were plotted on a cartesian plane. The loading rate was in any case such that fracture was achieved in about 1 minute.

Some load-displacement diagrams for mortar specimens are reported in figure 2. It is evident how the specimen stiffness decreases by increasing the crack depth.

3. EXPERIMENTAL DETERMINATION OF THE FRACTURE TOUGHNESS PARAMETERS

The critical values K_{IC} of the *stress-intensity factor* have been obtained applying, for each single test, the formula suggested by [6]. Such values have then been averaged, for each material and for each crack depth, and represented in figures 3. The extreme K_{IC} values for each crack depth have also been shown (*fig.* 3).

The mean K_{IC} value and its standard deviation for each material are reported in table I. Marble shows a fracture toughness higher than that shown by the cement materials. Among the latter the least tough was concrete 1, perhaps because of the high ratios (sand/cement) and (aggregate/cement) of its composition. The standard deviation for mortar was the lowest (5.30%), for marble and concrete 2 was acceptable (16.96 and 10.80% respectively), while for concrete 1 was very high (25.29%).

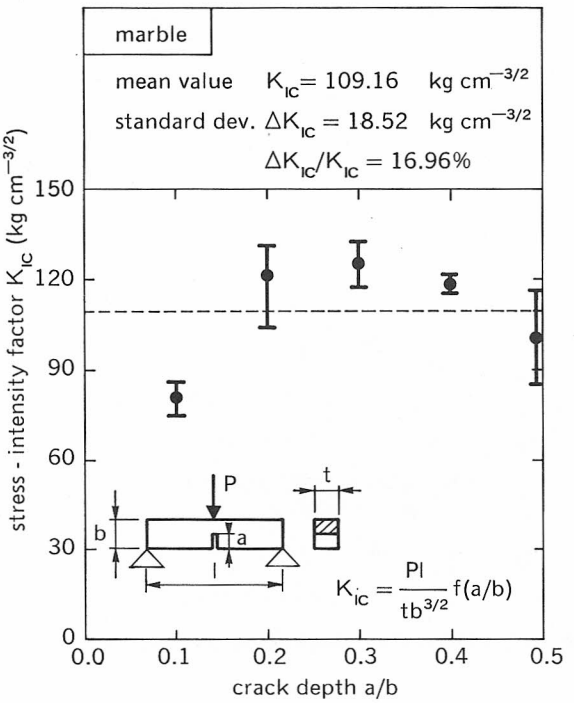

Fig. 3a. – Fracture toughness K_{IC} against relative crack depth (marble).

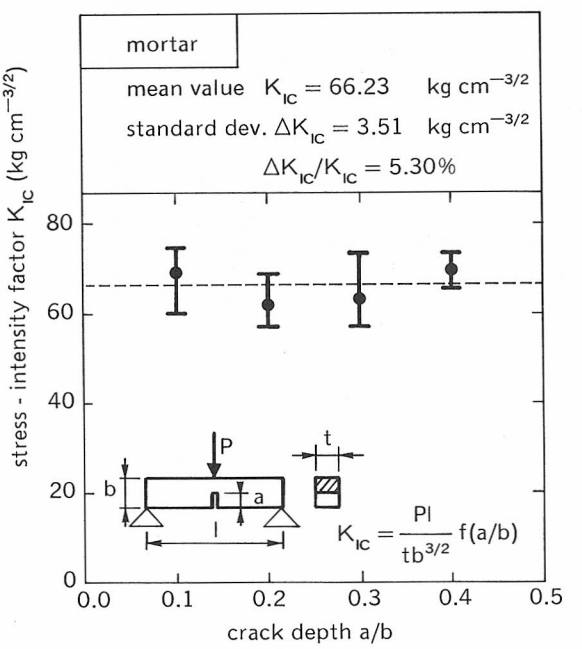

Fig. 3b. – Fracture toughness K_{IC} against relative crack depth (mortar).

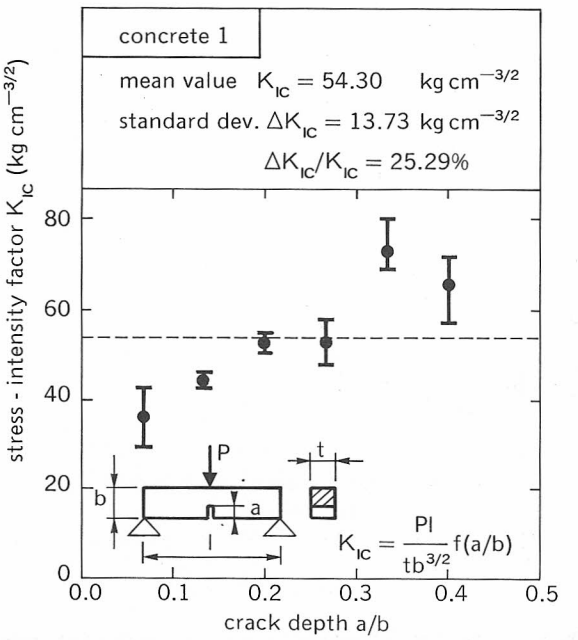

Fig. 3c. – Fracture toughness K_{IC} against relative crack depth (concrete 1).

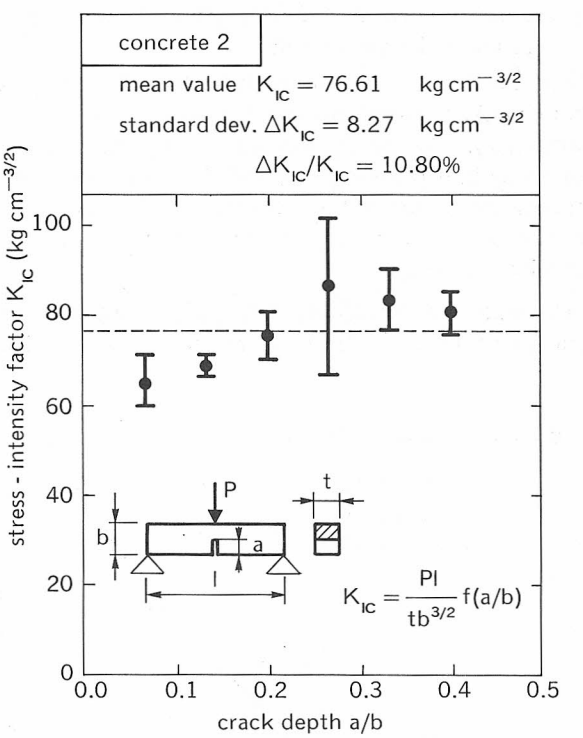

Fig. 3d. – Fracture toughness K_{IC} against relative crack depth (concrete 2).

Observing figures 3 the suspicion may arise that the mentioned deviations, more than by true statistical fluctuations, are caused by systematic errors. The factor K_{IC}, as a function of the relative crack depth, shows very similar and clear trends for marble and concretes: its values are increasing for low depths a/b and decreasing for higher depths. The tops of these diagrams are for $a/b = 0.25 \quad 0.30$.

The critical values $\mathcal{G}_{IC}$ of the *crack extension force* were obtained applying the formula [7]:

$$\mathcal{G}_I = -\frac{1}{2}\frac{P^2}{t}\frac{dC}{da}, \tag{1}$$

for every single crack length.

The variation dC/da of compliance with respect to crack length was obtained from the diagrams of figures 4,

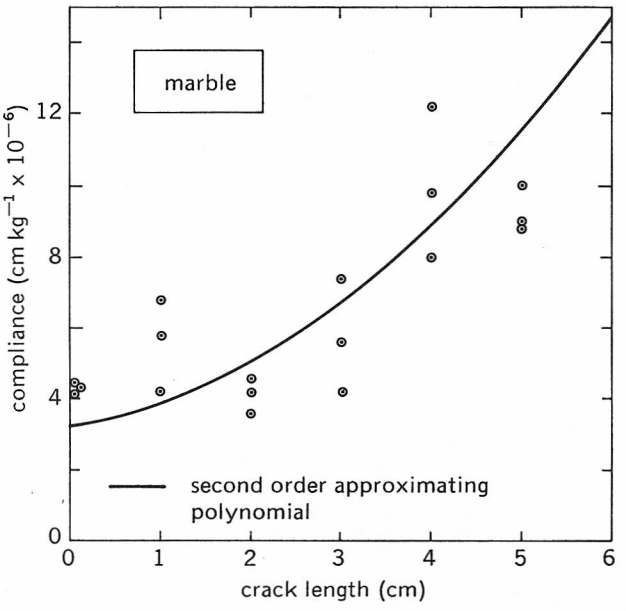

Fig. 4a. – Initial specimen compliance against crack length (marble).

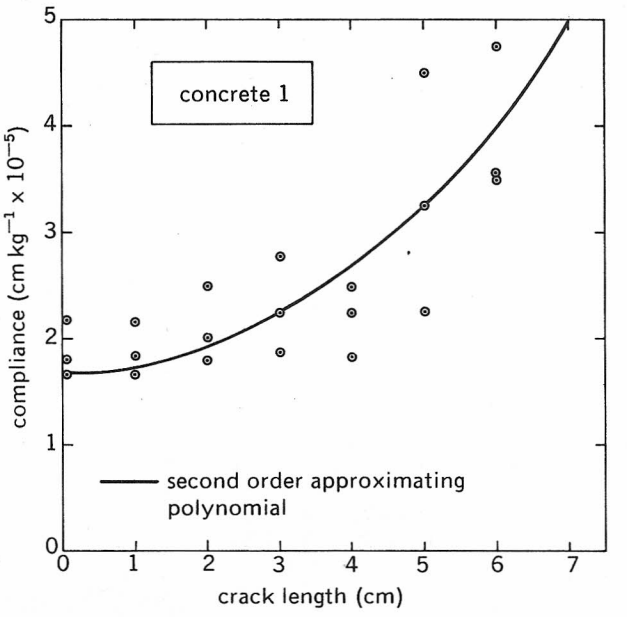

Fig. 4c. – Initial specimen compliance against crack length (concrete 1).

where the initial compliances of all the tests are represented against the crack length and approximated by a second order polynomial.

For marble and concretes bell-shaped curves were obtained like those previously shown (*fig.* 5-*a*, *c*, *d*). For mortar (*fig.* 5-*b*) the $\mathcal{G}_{IC}$ decreasing, by increasing the crack length, is probably due to the too low order of the approximating polynomial. Mortar has however revealed a crack extension force $\mathcal{G}_{IC}$ much higher than that of the other materials.

The standard deviations $\Delta\mathcal{G}_{IC}$ rightly appear higher than those of K_{IC}. In fact, recalling the quadratic relationship which connects K_{IC} and $\mathcal{G}_{IC}$ for a linear elastic material, it is possible to deduce that the standard deviations are connected by the following theoretical relationship:

$$\frac{\Delta\mathcal{G}_{IC}}{\mathcal{G}_{IC}} = 2\,\frac{\Delta K_{IC}}{K_{IC}}. \qquad (2)$$

The values of *J-integral* were calculated from load-displacement curves, following the procedure suggested by Begley and Landes [5] for steel alloys. At a given deflection δ the area under the load-displacement curves

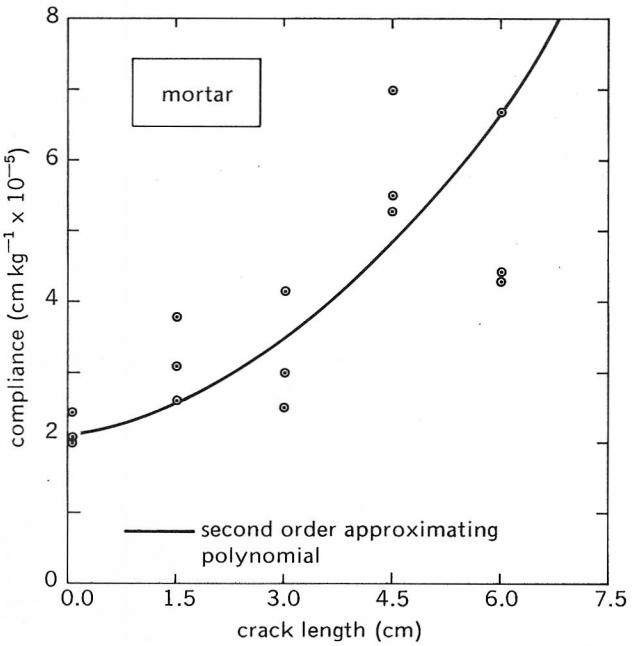

Fig. 4b. – Initial specimen compliance against crack length (mortar).

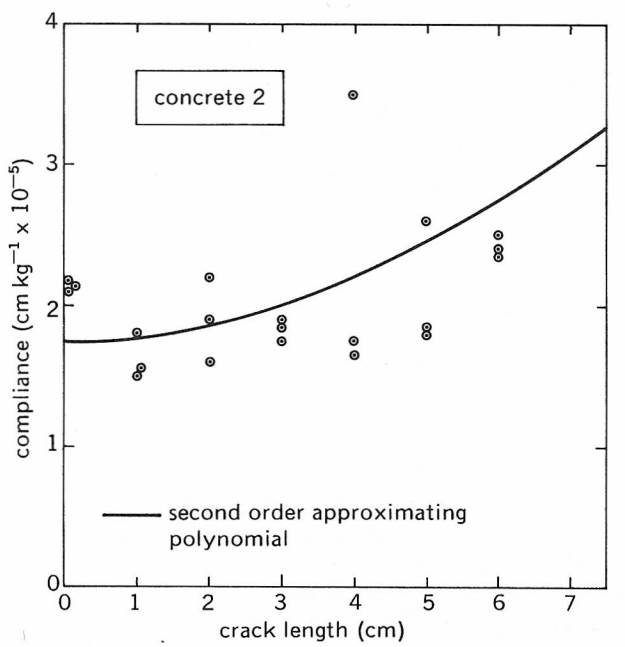

Fig. 4d. – Initial specimen compliance against crack length (concrete 2).

was recorded. Such energy at constant displacement was plotted as a function of crack length and fitted by straight lines with the method of least squares (*fig.* 6-*a*, *b*, *c*, *d*). The slope of these lines is equal to the variation in absorbed energy per unit variation in crack length and thus enables the determination of J as a function of deflection (*fig.* 7). It is supposed that J is directly a function only of deflection and not of crack depth. The last step of Begley-Landes' Method is the determination of the mean fracture deflection (*fig.* 8) and, then, of the critical value J_{IC} (*fig.* 7). In other words the generalized crack extension force J_{IC} was determined simulating the crack extension phenomenon by cracks of different length. For mortar J_{IC} also shows a value much higher than that of the other materials (table I). Observe how the standard deviation in fracture deflection, fluctuating for the four test series between 13.87 and 16.73%, is reflected and amplified in the J_{IC} value (table I).

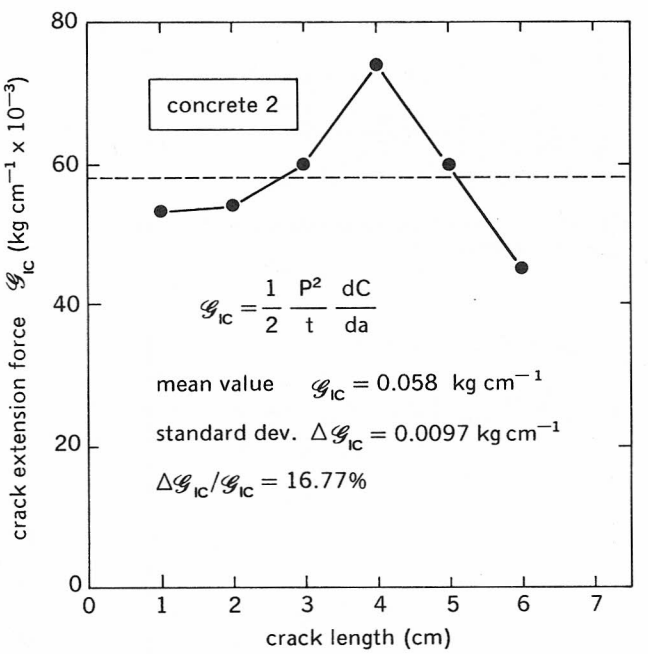

Fig. 5a. – Crack extension force $\mathcal{G}_{IC}$ against crack length (marble).

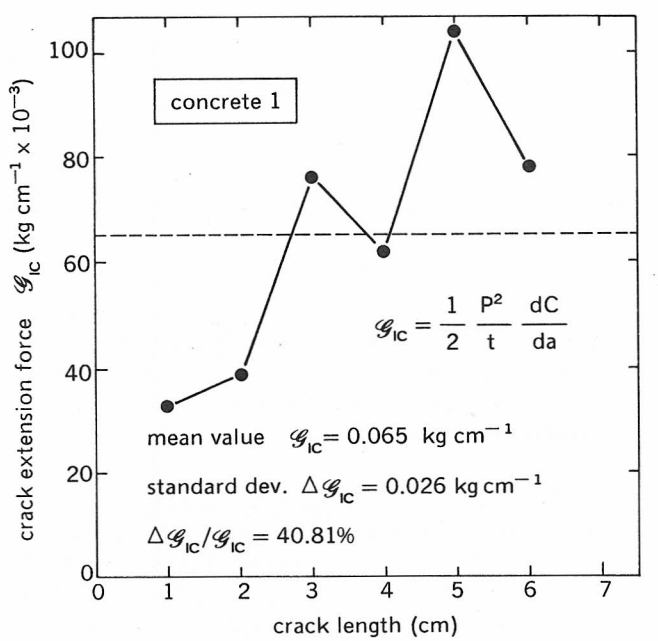

Fig. 5b. – Crack extension force $\mathcal{G}_{IC}$ against crack length (mortar).

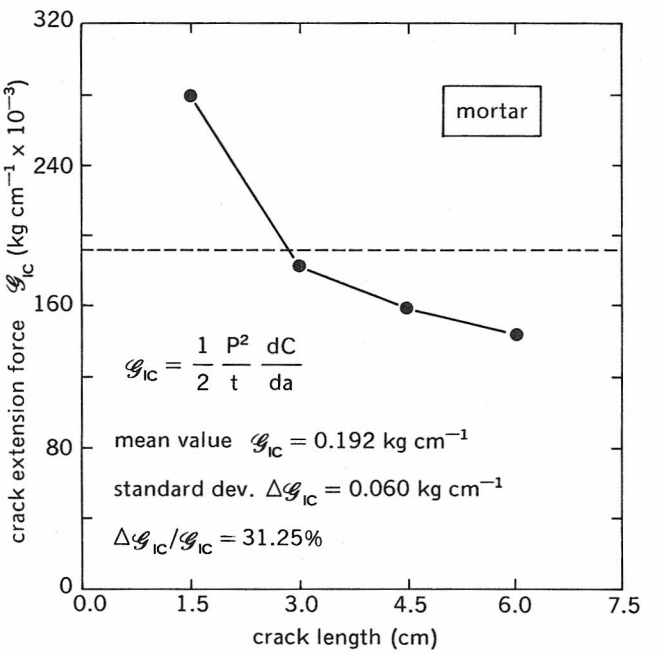

Fig. 5c. – Crack extension force $\mathcal{G}_{IC}$ against crack length (concrete 1).

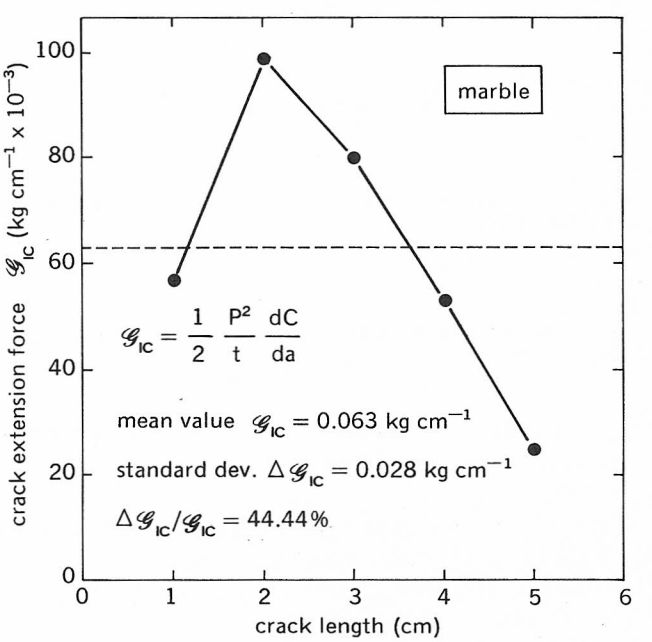

Fig. 5d. – Crack extension force $\mathcal{G}_{IC}$ against crack length (concrete 2).

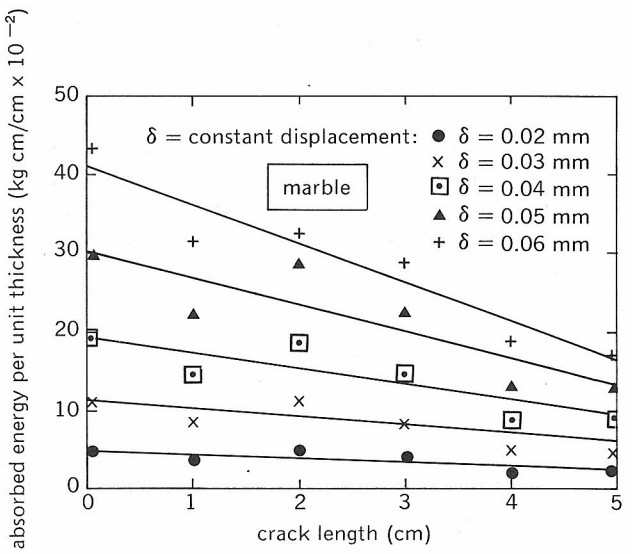

Fig. 6a. – Absorbed energy at constant displacement against crack length (marble).

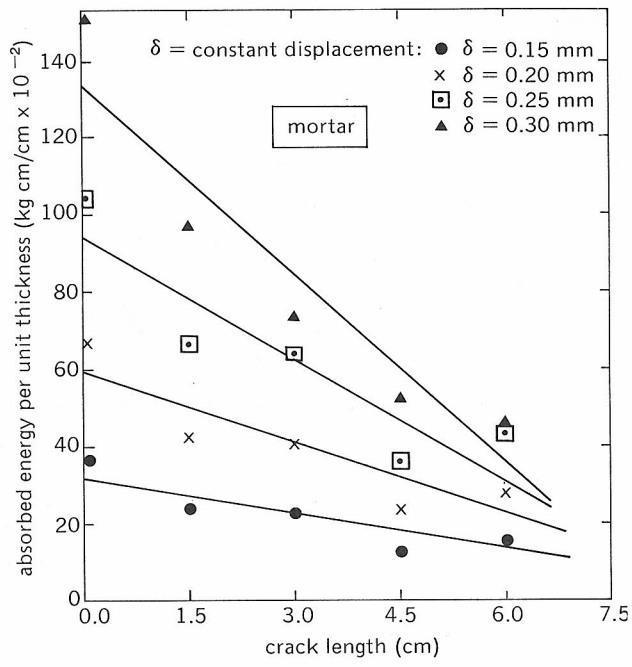

Fig. 6b. – Absorbed energy at constant displacement against crack length (mortar).

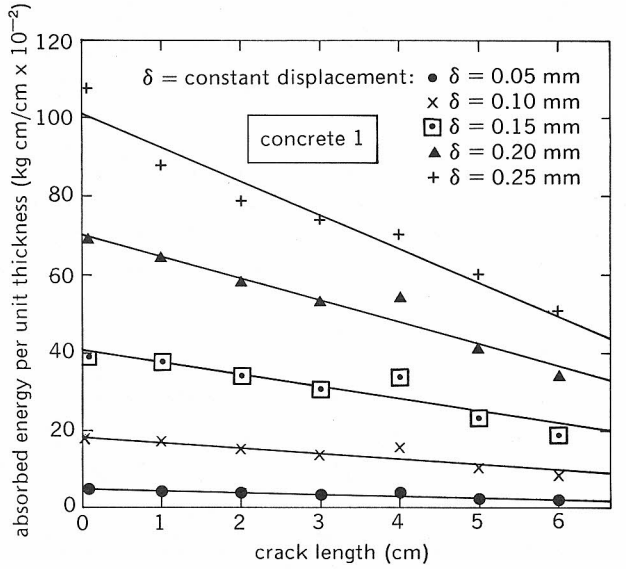

Fig. 6c. – Absorbed energy at constant displacement against crack length (concrete 1).

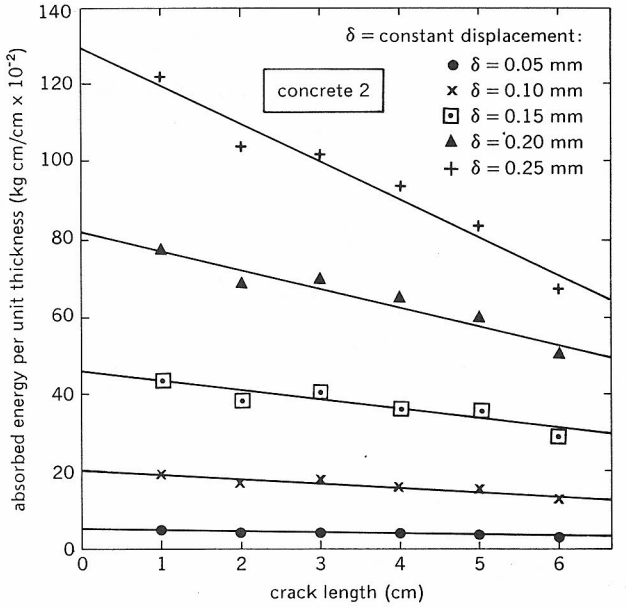

Fig. 6d. – Absorbed energy at constant displacement against crack length (concrete 2).

4. COMPARISON BETWEEN THE FRACTURE PARAMETERS OBTAINED

The critical values K_{IC}, $\mathcal{G}_{IC}$, J_{IC} and the standard deviations relating to the four materials are summarized in table I.

$\mathcal{G}_{IC}$ and J_{IC} should coincide for a linear elastic material. However when the material shows a non-linear behaviour, then the J_{IC} parameter, keeping in account the dissipative effects, i.e. the slope decrease in load-displacement diagram, should be higher than the $\mathcal{G}_{IC}$ parameter, which is defined in the linear field and thus keeping in account only the initial diagram slope. Only for mortar and concrete 2 does J_{IC} really appear higher than $\mathcal{G}_{IC}$. Probably it is due to the fact that appreciable non-linear effects revealed themselves only for two such materials.

On the other hand the difference between the two energetic parameters was very low (table I), emphasising the prevailingly linear and brittle behaviour of the aggregative materials.

A comparison between K_{IC} and J_{IC}, which have different physical dimensions, can be synthetically performed by considering the bending Young's

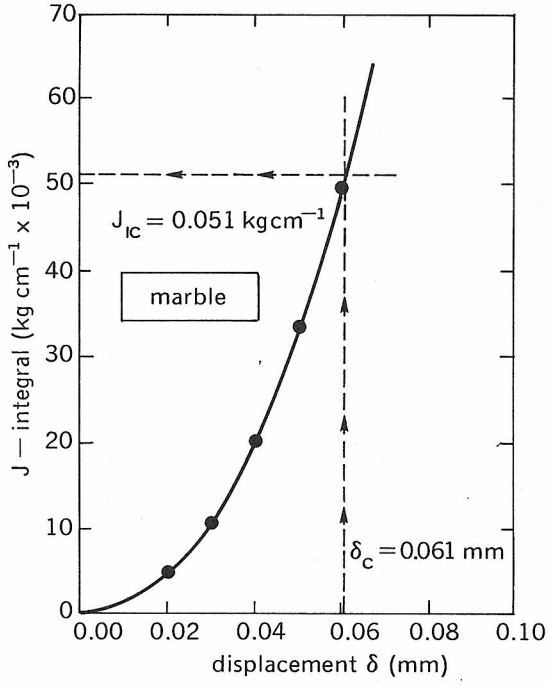

Fig. 7a. – *J*-integral as a function of displacement (marble).

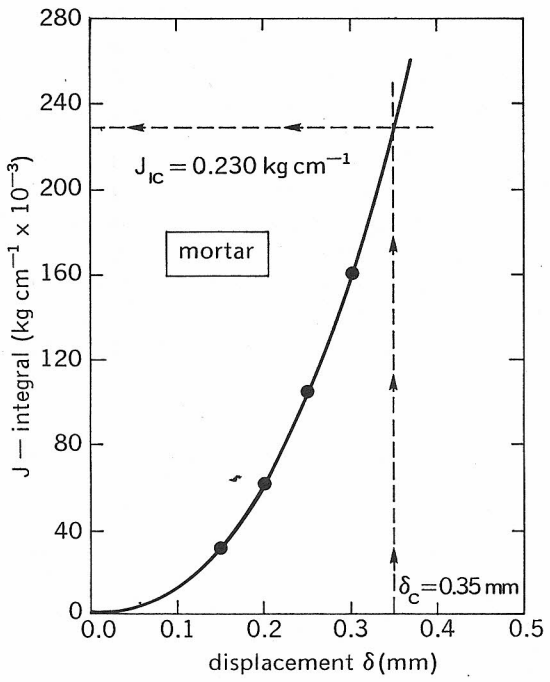

Fig. 7b. – *J*-integral as a function of displacement (mortar).

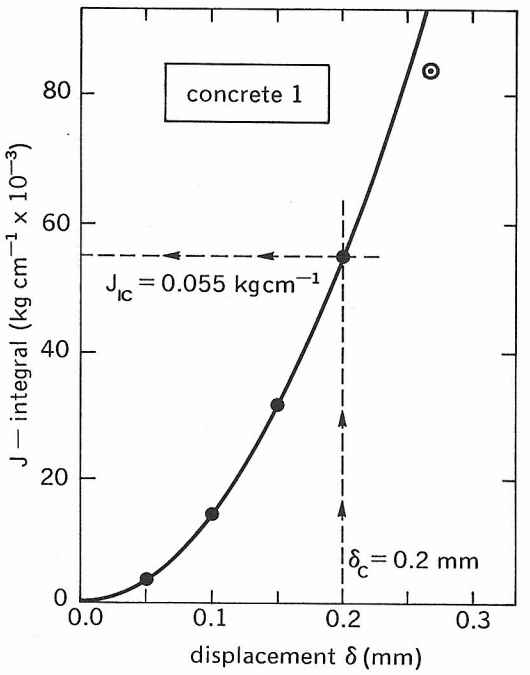

Fig. 7c. – *J*-integral as a function of displacement (concrete 1).

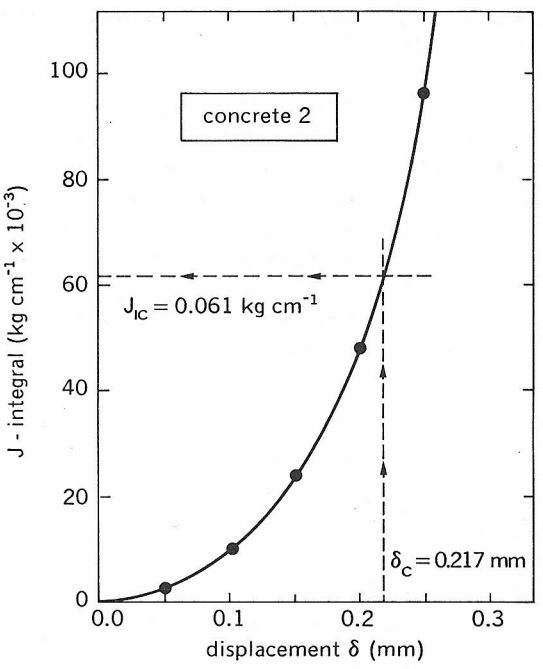

Fig. 7d. – *J*-integral as a function of displacement (concrete 2).

modulus E ([1]) and the fictitious Young's modulus:

$$E^* = K_{IC}^2 / J_{IC}. \tag{3}$$

For mortar the fictitious modulus E^* is about the half of E, while for marble and concretes E^* is much higher than E (table I). For mortar E^* could represent the stiffness of the damaged material near the crack tip before the extension. In the case of the remaining materials E^* could sound as an alarm and reveal too small a specimen size in order to obtain a real fracture collapse. In fact it is very improbable that a crack produces a stiffening of the material at its tip.

([1]) The bending Young's modulus E was obtained by the formula: $E = l^3/(4Ctb^3)$. That is the shear deflection was neglected.

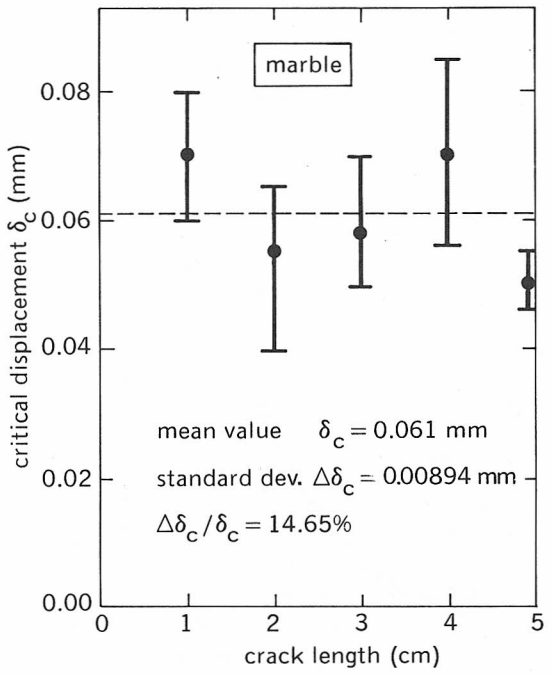

Fig. 8a. – Fracture deflection against crack length (marble).

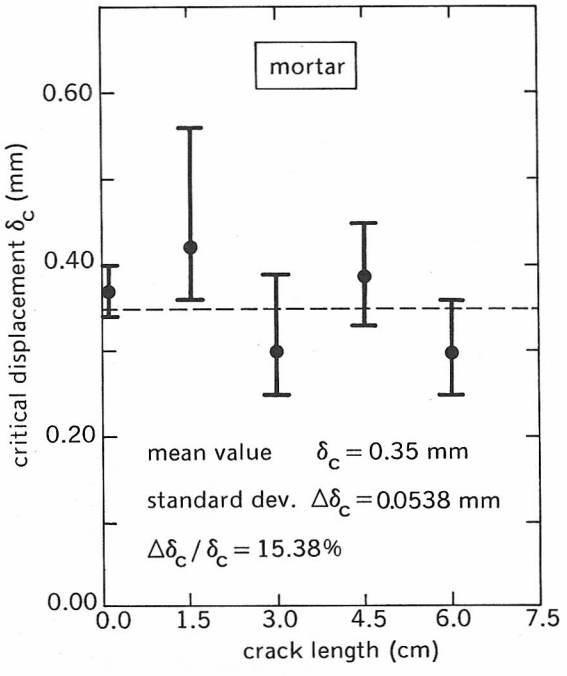

Fig. 8b. – Fracture deflection against crack length (mortar).

5. FRACTURE SENSITIVITY AND APPLICATION OF DIMENSIONAL ANALYSIS

A first idea of the fracture sensitivity can be provided by the ratio between the experimental load of failure and the calculated load of ultimate strength, relating to the cracked section. Such ratio is called *strength ratio;* when it is lower than unit it means that there is a stress concentration effect in addition to the section weakening effect. The strength ratio however depends on the specimen sizes, therefore it is not an absolute feature which also includes the size effects.

A stress concentration effect revealed itself for all the tested materials, as can be observed in figures 9, because of the considerable specimen sizes. A particularly regular diagram is that of mortar (*fig.* 9-*b*).

Based on the *Dimensional Analysis*, the author studied specimen and crack size effects on fracture testing of aggregative ([28], [29]) and metallic [30] materials. Such effects are due to the co-existence of two structural crises, induced by generalized forces with different physical dimensions ($\sigma = FL^{-2}$, $K_I = FL^{-3/2}$), and to the finiteness of specimen sizes. The application of

TABLE I

Material	Marble	Mortar	Concrete 1	Concrete 2
Specimen width, b (cm)	10	15	15	15
Ultimate strength, σ_u (kg.cm^{-2})	124.53	41.55	36.42	46.44
Bending Young's modulus, E (kg.cm$^{-2} \times 10^4$)	12.76	3.78	4.39	3.86
Stress-intensity factor, K_{IC} (kg.cm$^{-3/2}$)	109.16	66.23	54.30	76.61
Standard deviation, $\Delta K_{IC}/K_{IC}$ (%)	16.96	5.30	25.29	10.80
Crack extension force, $\mathcal{G}_{IC}$ (kg.cm^{-1})	0.063	0.192	0.065	0.058
Standard deviation, $\Delta\mathcal{G}_{IC}/\mathcal{G}_{IC}$ (%)	44.44	31.25	40.81	16.77
J-integral, J_{IC} (kg.cm^{-1})	0.051	0.230	0.055	0.061
Standard deviation, $\Delta J_{IC}/J_{IC}$ (%)	29.41	30.40	27.30	36.06
$(J_{IC} - \mathcal{G}_{IC})/J_{IC}$ (%)	−23.53	+16.52	−18.18	+4.92
Fictitious Young's modulus, E^* (kg.cm$^{-2} \times 10^4$)	23.36	1.91	5.36	9.62
Brittleness number, $K_C^{(r)}/\sigma_u b^{1/2}$	>0.32	0.41	>0.52	>0.48

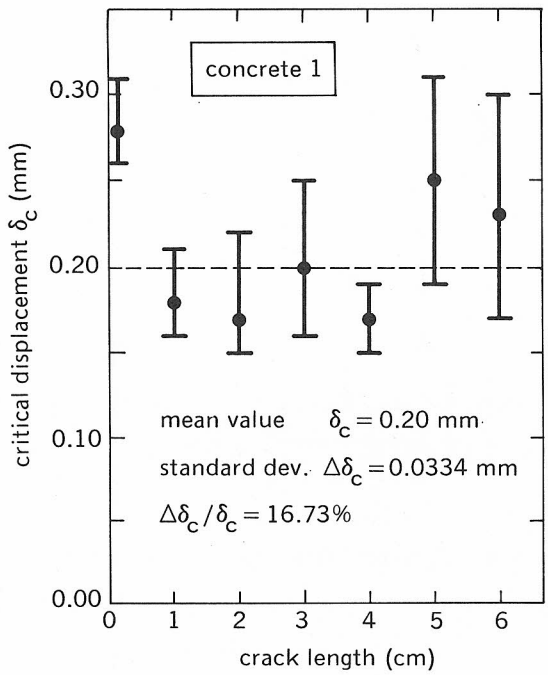

Fig. 8c. – Fracture deflection against crack length (concrete 1).

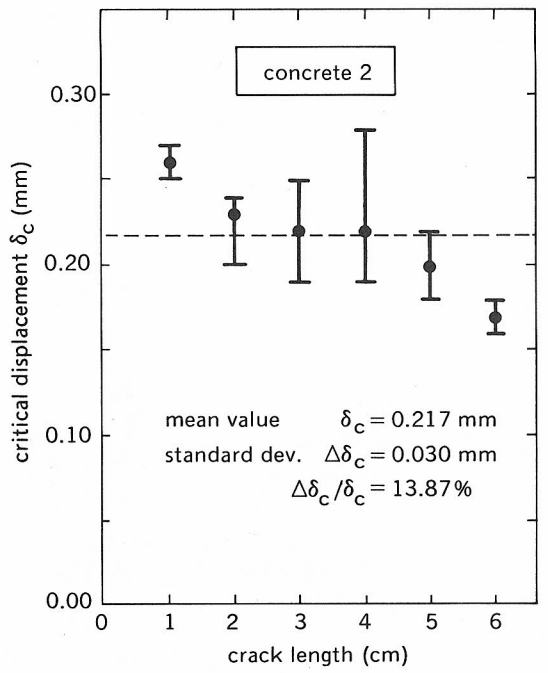

Fig. 8d. – Fracture deflection against crack length (concrete 2).

Buckingham's Theorem allows the definition of a non-dimensional parameter s, which governs the fracture sensitivity phenomenon. Some recurring experimental incoherences are thus explained, such as the increase or decrease of fracture toughness K_{IC} increasing the crack length, the increase of K_{IC} increasing the specimen sizes, the variability of K_{IC} varying the test geometry.

Let q_0 be the failure load, for ultimate strength overcoming and/or for crack propagation, in a cracked structure. In the simplest case of homogeneous, isotropic and linear elastic material it is possible to show [28]:

$$q_0/\sigma_u^{\alpha} b^{\beta} = \varphi_1(s, a/b)\,\varphi_2(t/b, l/b), \tag{4}$$

where φ_1 is a function of the *brittleness number:*

$$s = \frac{K_{IC}}{\sigma_u b^{1/2}}, \tag{5}$$

and of the relative crack depth a/b, and b, l and t are the sizes of the body. The actual function φ_1 depends on the material stress-strain laws and could be exactly determined only by experience. However an upper bound to φ_1 can be utilized, for example in the case of the three point bending test. The non-dimensional fracture load against the relative crack length, varying the brittleness number s, is reported in figure 10, together with the ultimate strength load. It is evident how the fracture tests completely lose their meaning for $s \gtrsim 0.50$. For $s \lesssim 0.50$ the fracture tests are significant only with cracks of intermediate length. Diagrams of figure 10 would represent the real φ_1 only if the ultimate strength collapse were independent of the fracture collapse. Really the two collapses are interacting: that is, by decreasing the specimen sizes, fracture collapse becomes ultimate strength collapse, passing through mixed collapses.

"Mixed collapse" means that the crisis mechanism is the overcoming of the ultimate strength rather than the crack propagation, but the specimen is sufficiently large to feel stress concentration effects.

The bell-shaped diagrams of K_{IC} obtained for marble and concretes (*fig.* 3-*a*, *c*, *d*) reveal that the crisis has prevailingly occurred for ultimate strength overcoming. It is interesting to observe how the top of these diagrams corresponds to the value a/b, for which the fracture curve $s = 0.50$ is tangent to the ultimate strength curve (*fig.* 10). Therefore for marble and concretes the collapse was of mixed type, i.e. it occurred for material cohesion lost rather than for crack propagation.

However, in the case of mortar, the low statistical fluctuations of K_{IC} and the lack of a bell-shaped variation show that the crisis occurred for crack extension.

The experimental value $K_{IC} = 66.23\ \mathrm{kg.cm^{-3/2}}$, obtained for mortar, should be the real one. For the other materials the real value $K_{IC}^{(r)}$ should however be higher than the mean value reported in table I, and, indeed, it should be higher than the maximum value of the bell-shaped diagrams $K_{IC}(a/b)$ (*fig.* 3-*a*, *c*, *d*). Therefore it is possible to determine the test brittleness number for mortar, and to set a lower bound to the numbers of the remaining tests (table I).

6. CONCLUSIONS

In fracture testing of several materials, even metallic, the dimensional effects have not been considered. For too small specimens and for too short [31] or too long cracks the collapse is at least partially to charge to the material cohesion lost (or to the plastic flow).

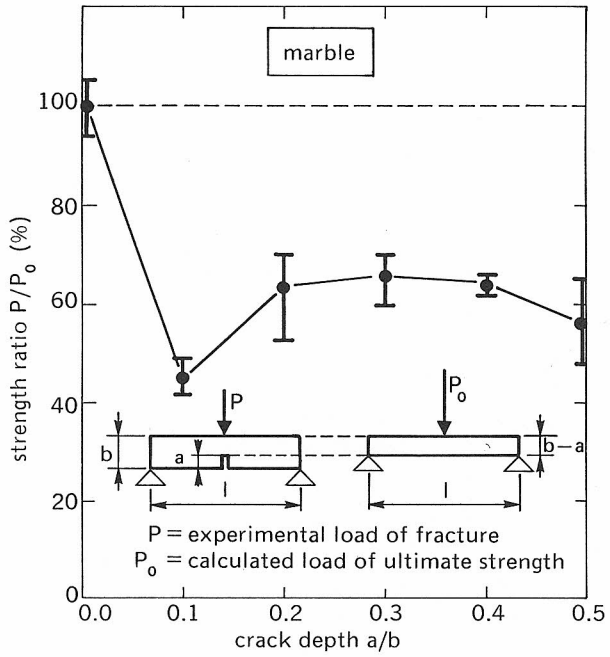

Fig. 9 a. – Strength ratio against relative crack depth (marble).

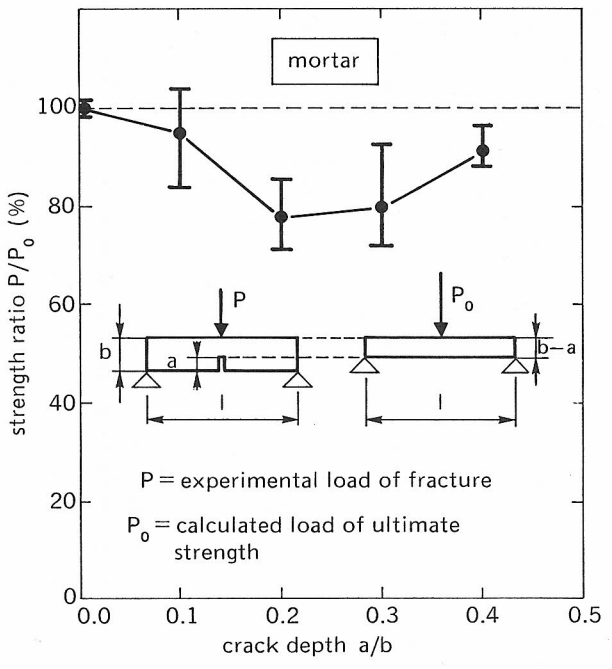

Fig. 9 b. – Strength ratio against relative crack depth (mortar).

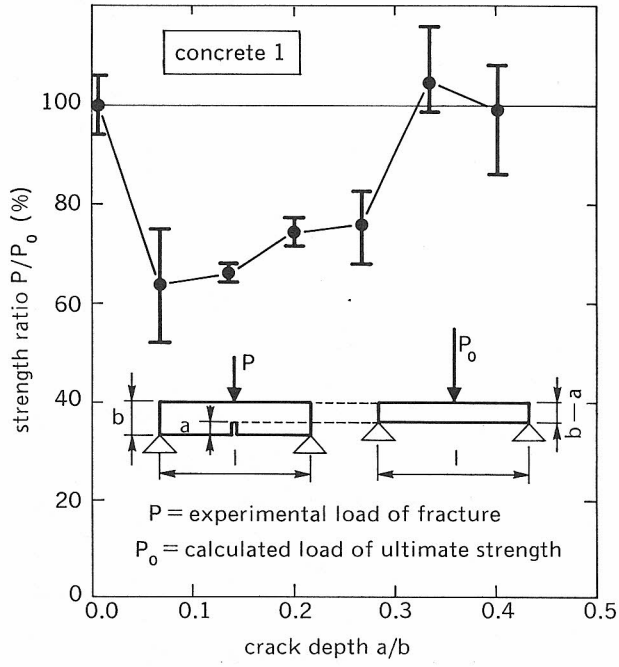

Fig. 9 c. – Strength ratio against relative crack depth (concrete 1).

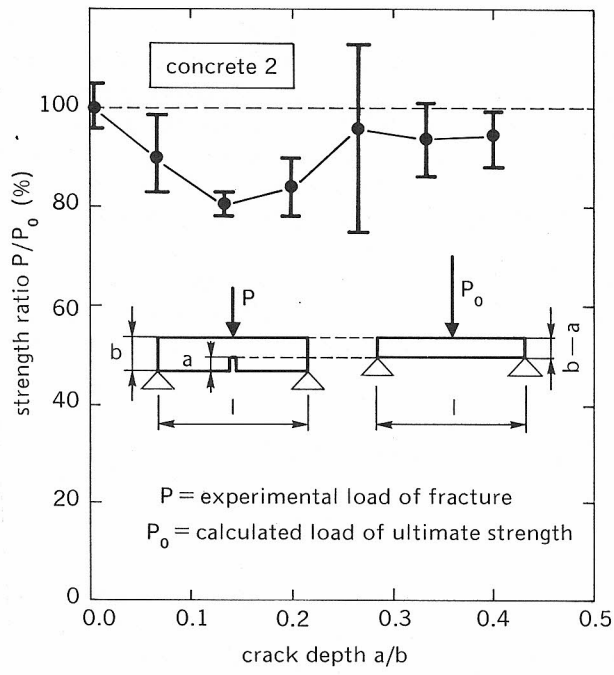

Fig. 9 d. – Strength ratio against relative crack depth (concrete 2).

The crack propagation is the sole cause of collapse only for sufficiently large structures. An evident confirmation of this assertion is provided by the innumerable sudden failures, occurred in always large structures and due to relatively small cracks.

Those collapses of dams, bridges, ships, which are referenced here, occurred in a completely brittle way, i. e. without remarkable plastic strain pre-announcing the impending failure. The same materials show much less linear behaviours in similar but smaller structures, and their collapse is not so catastrophic.

For the metallic alloys such phenomenon has been empirically explained, by observing that the crack tip plastic zone at failure has always about the same extension, and then it works as a brake only for sufficiently small structures.

As far as the aggregative materials are concerned, for which the plastic effects are lacking, the explanations have been less convincing: as has been said, the microcracking and the slow crack growth have been taken into consideration. The fact that a cracked specimen appears much tougher than a cracked large

structure of the same material, should then depend on the fundamental laws of physical similitude rather than on collateral effects, such as the relative decrease of plastic zone, the increase of stress triaxiality or the increase of stress raiser number, with increasing size.

Fracture sensitivity is a usual phenomenon being part of our everyday experiences. For example adhesive tape and cloth are extremely notch sensitive materials: they need terrible stresses to be broken, but, just performed a little lateral notch, this can be extended with a very low stress.

It is due to the low ratio K_{IC}/σ_u, which makes these materials notch-sensitive, even for the usual widths of adhesive tape or cloth rolls. If materials with a much higher ratio K_{IC}/σ_u are considered, as for example concretes or steel alloys, a similar situation can be produced again only with very large sizes, so as to obtain brittleness numbers s of the same magnitude. Thus a concrete dam can be completely similar to an adhesive tape in the sense of the physical fracture behaviour. At the basis of such a *brittleness for size increasing* there is perhaps only an homogeneity effect.

In the tests performed by the author a fracture collapse seems to have occurred only for mortar, because of the

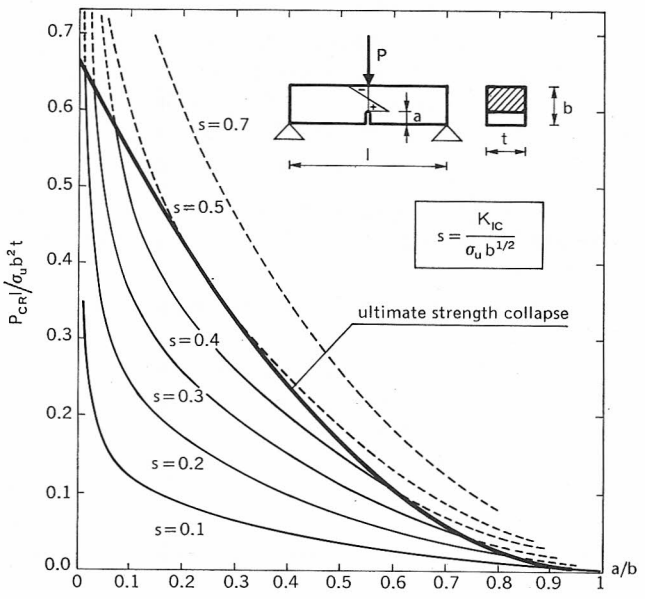

Fig. 10. – Fracture load and ultimate strength load as functions of relative crack depth.

low ratio K_{IC}/σ_u of such material and the sufficiently large specimen sizes. This assertion is supported by four symptoms in mortar tests:

1) the regularity of the strength ratio (and its statistical fluctuations) as a function of the crack length (*fig. 9-b*);

2) the low standard deviation of K_{IC} and the lack of a bell-shaped variation (*fig. 3-b*);

3) the toughness parameter J_{IC}, considering also the plastic effects, is higher than $\mathcal{G}_{IC}$, holding only in the linear elastic field (table I);

4) the fictitious Young's modulus E^* is lower than the bending Young's modulus E (table I).

Being the maximum aggregate size larger than the crack tip radius, for the specimens of mortar and concrete used by the author, it is probable that the crack has revealed itself sufficiently sharp. Perhaps the same cannot be said about the marble, which is a more homogeneous material. A dimensional analysis including the crack tip radius effects on fracture, could however be carried out.

ACKNOWLEDGMENT

The author gratefully acknowledges the research support of the National Research Council (C.N.R.).

REFERENCES

[1] IRWIN G. R. – *Analysis of stresses and strains near the end of a crack traversing a plate*, J. Appl. Mech., Vol. 24, 1957, pp. 361-364.

[2] GRIFFITH A. A. – *The phenomenon of rupture and flow in solids*, Proc. Ist. Int. Congr. Appl. Mech., 1924.

[3] RICE J. R. – *A path independent integral and the approximate analysis of strain concentration by notches and cracks*, J. Appl. Mech., Vol. 35, 1968, pp. 379-386.

[4] RICE J. R. – *Mathematical analysis in the mechanics of fracture*, Fracture, Liebowitz, Ed., Vol. III, 1968, pp. 191-311.

[5] BEGLEY J. A., LANDES J. D. – *The J-integral as a fracture criterion*, ASTM STP Vol. 514, 1972, pp. 1-23.

[6] *Standard method of test for plane strain fracture toughness of metallic materials*, E 399-74, ASTM.

[7] KAPLAN M. F. – *Crack propagation and the fracture of concrete*, ACI Journal, Vol. 58, No. 11, November 1961, pp. 591-610.

[8] ROMUALDI J. P., BATSON G. B. – *Mechanics of crack arrest in concrete*, J. Eng. Mech. Div. (ASCE), June 1963, pp. 147-167.

[9] GLUCKLICH J. – *Fracture of plain concrete*, J. Eng. Mech. Div. (ASCE), December 1963, pp. 127-136.

[10] NAUS D. J., LOTT J. L. – *Fracture toughness of Portland cement concretes*, ACI Journal, June 1969, pp. 481-489.

[11] WELCH G. B., HAISMAN B. – *The application of fracture mechanics to concrete and the measurement of fracture toughness*, Matériaux et Constructions, Vol. 2, No. 9, 1969, pp. 171-177.

[12] MOAVENZADEH F., KUGUEL R. – *Fracture of concrete*, J. of Materials, Vol. 4, No. 3, 1969, pp. 497-519.

[13] DESAYI P. – *Fracture of concrete in compression*, Matériaux et Constructions, Vol. 10, No. 57, 1969, pp. 139-144.

[14] SHAH S. P., MCGARRY F. J. – *Griffith fracture criterion and concrete*, J. Eng. Mech. Div. (ASCE), December 1971, pp. 1663-1675.

[15] BROWN J. H. – *Measuring the fracture toughness of cement paste and mortar*, Magazine of Concrete Research, Vol. 24, No. 81, 1972, pp. 185-196.

[16] NAUS D. J., BATSON G. B, LOTT J. L. – *Fracture mechanics of concrete*, Fracture Mechanics of Ceramics, Bradt, Hasselman, Lange, Eds., Vol. 2, 1974, pp. 469-481.

[17] WALSH P. F. – *Crack initiation in plain concrete*, Magazine of Concrete Research, Vol. 28, 1976, pp. 37-41.

[18] HIGGINS D. D., BAILEY J. E. – *Fracture measurements on cement paste*, J. Materials Science, Vol. 11, 1976, pp. 1995-2003.

[19] SCHMIDT R. A. – *Fracture-toughness testing of limestone*, Experimental Mechanics, May 1976, pp. 161-167.

[20] BEAR T. J., BARR B. – *Fracture toughness tests for concrete*, Int. Journ. of Fracture, Vol. 13, 1977, pp. 92-96.

[21] BARR B., BEAR T. – *A simple test of fracture toughness*, Concrete, 25-27, April 1976.

[22] BARR B., BEAR T. – *Fracture toughness*, Concrete, 30-32, april 1977.

[23] HENRY J. P., PAQUET J. – *La ténacité des roches calcaires : influence des parametres microstructuraux et de l'environnement*, Mech. Res. Comm., Vol. 4, (3), 1977, pp. 193-198.

[24] HENRY J. P., PAQUET J. TANCREZ J. P. – *Experimental study of crack propagation in calcite rocks*, Int. J. Rock Mech. Min. Sci. & Geomech., Vol. 14, 1977, pp. 85-91.

[25] HENRY J. P., PAQUET P. – *Résistance des matériaux*, C. R. Acad. Sc. Paris, T. 284, 1977, pp. 511-514.

[26] HILLEMEIER B., HILSDORF H. K. – *Fracture mechanics studies on concrete compounds*, Cement and Concrete Research, Vol. 7, 1977, pp. 523-536.

[27] STRANGE P. C., BRYANT A. H. – *Experimental tests on concrete fracture*, J. Eng. Mech. Div., April 1979, pp. 337-342.

[28] CARPINTERI A. – *Notch sensitivity in fracture testing of aggregative materials*, Eng. Fracture Mech. (to appear).

[29] CARPINTERI A. – *Experimental determination of fracture toughness parameters K_{IC} and J_{IC} for aggregative materials*, Proc. Fifth Int. Conf. on Fracture, Cannes, 1981.

[30] CARPINTERI A. – *Size effect in fracture toughness testing: a dimensional analysis approach*, Proc. Int. Conf. on Analytical and Experimental Fracture Mechanics, G.C. Sih, Ed., Roma, 1980.

[31] CARPINTERI A., DI TOMMASO A., VIOLA E. – *Collinear stress effect on the crack branching phenomenon*, Materials and Structures (RILEM), Vol. 12, No. 72, 1979, pp. 439-446.

RÉSUMÉ

Les paramètres statiques et énergétiques de rupture des roches et des bétons. – *On a cherché à établir les paramètres de résilience K_{IC}, $\mathcal{G}_{IC}$ et J_{IC} d'un carrare, d'un mortier et de deux bétons dont les granulats ont différentes dimensions maximales. L'essai choisi a été l'essai de flexion sur deux points d'appui. Les valeurs du paramètre énergétique « J-intégral » ont été obtenues d'après les courbes charge-déplacement, selon le procédé appliqué par Begley et Landes aux aciers alliés.*

On explique des incohérences expérimentales à caractère récurrent à l'aide du théorème de Buckingham, pour ce qui concerne la similitude physique et les modèles en échelle. Par conséquent, l'on établit un paramètre non dimensionnel (fragilité à l'essai), qui régit le phénomène de sensibilité à la rupture.

La connexion des paramètres de rupture K_{IC} et J_{IC} est obtenue grâce à un module de Young fictif, E^*, qui est inférieur au module réel E et qui représente la valeur de la rigidité du matériel détérioré à proximité de la fissure avant sa progression. E^* s'avère supérieur à E quand la taille de l'éprouvette de traction est à tel point réduite que le matériel devient insensible à la rupture.

Une rupture par propagation de la fissure semble s'être produite seulement dans le cas du mortier, à cause du faible rapport K_{IC}/σ_u de ce matériel et de la taille assez importante de l'éprouvette. Quatre indices mis en évidence au cours des essais sur le mortier le confirment :

1) *le caractère régulier du « strength ratio » et des fluctuations d'un point de vue statistique, en fonction de la longueur de la fissure;*

2) *le faible écart type de K_{IC} qui ne montre pas de variation en cloche;*

3) *le paramètre J_{IC}, qui comprend aussi les effets plastiques, est supérieur à G_{IC}, qui n'intervient que dans le domaine élastique (linéaire);*

4) *le module de Young fictif E^* est inférieur au module réel E.*